Force and Energy Balances on Towed Platforms which Approach Flat Plate Airfoil Performance

by Galen J. Suppes, PhD, P.E.
February, 2021.

INTELLECTUAL MERITS

The Innovation – Ongoing efforts by major players on the D8 Double Bubble and Blended-Body-Wing concepts[1, 2] substantiates that there is unrealized potential per increased use of lifting body technology. Drone aircraft start at lower performances, have lower barriers, and increased upside potential (e.g. VTOL) than airliners; electric VTOL aerial drones are the emphasis of this project.

The Initial Innovation – Transformer Drone's initial, and patented, technology is a VTOL drone multicopter with a front tiltwing in front of a fuselage; wherein, the transition to cruising includes forming an effective lifting-body "Liftpath" that extends the length of the drone. To understand and realize the potential of lifting body technology requires a review of the lifting body technology starting with the geometric mandates of that science.

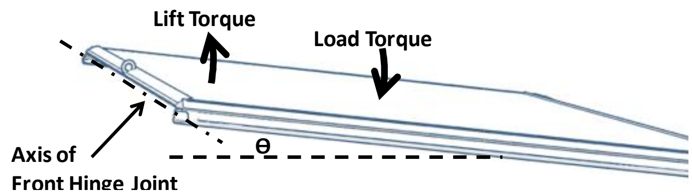

Figure 9. Illustration of towed flat plate platform pivotable about a front hinge joint.

Figure 11. Side cross section of practical flat plate airfoil.

Summary of Science per Appendix A – A more-in-depth technical discussion is provided as an Appendix A to preserve the flow of presentation of the innovations. Summary of key points of the theory, calculations, and heuristics of Appendix A are as follows:

- The towed platform is a key feature of SP-Drone and some fuselages of Transformer Drone; it is approximated as a flat plate airfoil as illustrated by Figure 9.
- Very high L:D (>100:1, see Figure 10) are a "geometric mandate", where the challenge is to maintain stable flight at 0.2° < θ < 1.0°.
- Whereas power needs are proportional to v^3 for typical wing airfoils, a better estimate for the flat plate airfoil is power proportional to velocity (v), which makes high velocity flight more feasible/preferred for towed platforms.
- A practical flat plate airfoil (see Figure 11) has a cambered leading edge that rapidly develops desired pressure profiles in the direction of air flow; that leading edge is a disproportionate source of drag, but it is critical for high performance.
    - **The Innovations** – A critical analysis of the science reveals a "sweet spot" of operation to achieve very high L:D. Transformer Drone has passed the patent office (USPTO) scrutiny as a novel approach with tiltwings transform to part of larger lifting-body lift surfaces. The towed platform has a synergy with the Transformer Drone transformations to achieve high levels of performance consistent with a variety of drone applications.

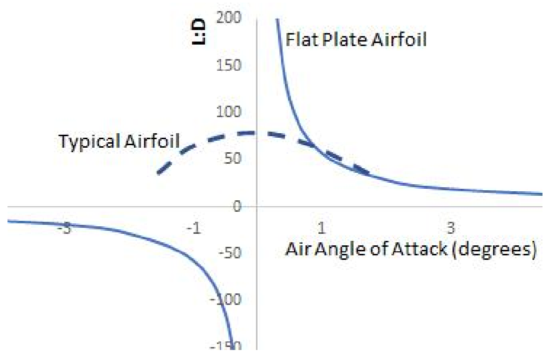

Figure 10. L:D of flat plate airfoil and a typical wing airfoil.

APPENDIX A: THEORY, DERIVATIONS, CALCULATIONS (WITHIN PAGE LIMIT)

Geometric Mandates of Lifting Body Technology – For steady-state flight, a force balance can be performed on the surface of an aircraft to estimate lift and drag. Shear drag can be neglected for L:D up to at least 50:1;[1] and so, lift and drag can be approximated by the following two surface integrals:

$$L = \oint n_V \Delta P dS = \sum \oint n_{V,i} \Delta P dS\,; \quad D = \oint n_H \Delta P dS = \sum \oint n_{H,i} \Delta P dS \tag{1}$$

where: ***L*** is lift, ***D*** is drag, ***P*** is pressure, ***n*** is a unit vector in ***V***ertical or ***H***orizontal direction, ***S*** is surface. The summation identifies that the integral can be the sum of integrals for the parts. A takeaway is that the same ***ΔP*** (surface pressure minus ambient pressure) drives both lift and drag.

For L:D of a flat plate airfoil: the unit vectors are constant and both ***ΔP*** and ***S*** cancel in the ratio. This results in L:D = θ^{-1} where ***θ*** is air's angle (radians) of attack in the limit of low air angle of attacks (i.e. for near-horizontal inclination).[3-7] Example L:D are 57:1 at 1° and 114:1 at 0.5°. There high L:D are <u>geometric mandates</u> contingent on: a) negligible shear drag and b) being able to maintain stable flight at these low values of ***θ***.

Negligible shear drag is a reasonable for streamlined surfaces at L:D < 50:1; and is primarily a moderate correction at values up to about 150:1. A potential source of higher shear drag is turbulence associated with boundary layer separation, but boundary layer separation should not be a problem at low ***θ***. An energy analysis and heuristics allows these L:D to be used to estimate performance.

Energy Balance – The energy balance for air can be derived from fundamentals for the series of equations shown by Equation 2.

$$0 = 0.5\,\dot{m}\frac{dv^2}{dz} + \dot{m}\frac{dH}{dz}\,; \qquad 0.5\,v_{max}^2 = -C_p \Delta T\,; \qquad \left(\frac{T_2}{T_1}\right) = \left(\frac{P_2}{P_1}\right)^{(\gamma-1)/\gamma} \tag{2}$$

where ***H*** is enthalpy, ***m*** is mass, ***v*** is velocity, ***z*** is distance orthogonal to surface, v_{max} is the air foil velocity, ***T*** is temperature, and C_P is heat capacity. The "***max***" subscript of Equation 2 assumes all kinetic energy is transformed to lift. When integrated, the velocity component that actually enters the control volume is ***θv*** at small ***θ***, and so, ***ΔP*** is a function of θv^2_{max}.

The Equation 2 derivation is based on adiabatic isentropic assumption and provides a result within 4% of the incompressibility function used to derive the simpler Bernoulli equation for maximum ***ΔP***, absent the ***θ*** correction, per Equation 3.[8]

$$0.5\ (\rho\, v_{max}^2) = \Delta P \qquad (\rho \text{ is density}) \tag{3}$$

The Equation 2 series was used to estimate specific lift (lb/ft2) as summarized by Table 4.

Table 4. Maximum specific loads supported on towed platforms. The Specific Lifts are the sum of upper and lower lift surfaces.

			ΔP = Specific Lift = Specific Load (lb/ft²)					
			P = 1.0 atm			P = 0.1 atm		
Velocity		θ(°)	0.1	1	5	0.1	1	5
(kph)	(mph)	L:D	573	57	11	573	57	11
50	31		0.52	5.24	26.2	0.052	0.52	2.62
100	62		2.10	21.0	105	0.210	2.10	10.5
200	124		8.50	85.0	425	0.85	8.5	42.5
500	311		57	571	2857	5.71	57.1	286
900	559		224	2239	11193	22.39	223.9	1119

Sweet Spot – The "sweet spot" of operation is a range; it is a combination of specific loads and velocities resulting in high L:D (i.e. 0.2° < ***θ*** < 1.0°).[2]

As discussed in the next few paragraphs, the maximum specific loads of Table 4 are about twice what can be reasonable achieved. And to put things into perspective, typical passenger jet takeoff velocities are 150 to 180 mph with wing loadings of 100 to 150 lb/ft² and smaller prop aircraft have specific loads up to about 70 lb/ft². <u>That is why this geometric mandate has not been studied more.</u>

Heuristic on Approach to Table 4 Maximum Specific Lifts – The equation 1 surface integral inherently relates drag to lift through pressure, and so, a drag coefficient can be used as a heuristic correction to Equations 2 and 3. Equation 4 presents the drag coefficient equation for which drag coefficients (C_d) have been extensively measured.

$$D = 0.5\ A_{FCS}\, C_d\, (\rho\, v_{max}^2) \qquad (A_{FCS} \text{ is Frontal Cross Section Area}) \tag{4}$$

---

[1] The shear drag in form of a coefficient is 0.001. The eta glider has an L:D of 70:1 and is a practical example of form drag dominating the drag term.

[2] Two pressures are provided in Table 4, one for runway takeoff/landing and one for cruising. Runway takeoff/landing is irrelevant for VTOL.

Aircraft use their wing area as the reference area when computing, while automobiles (and many other objects) use frontal cross-sectional area. Here, the frontal cross-section approach is more useful because its range is typically 0.35 to 0.45 (a more-limited range). This value depends upon how the streamlined shape is able to deflect/reroute the maximum velocity; the more the deflection the lower the coefficient. For an infinitely large flat plate, the drag coefficient would be 1.0. For a flat plate airfoil with fences that block the air from being deflected/rerouted, values greater than the 0.35 to 0.45 range are possible. A reasonable heuristic of attainable values of L:D is C_d=0.5, which translates to being able to attain half the specific loads listed in Table 4.

Towed Solar Platform - Figure 9 illustrates the towed platform where lift torque balances load torque in passive stability.[9] Solar cells are available at less than 0.16 lb/ft^2 [10] and corrugated plastic is available at less than 0.15 lb/ft^2. For this platform a sheet of metal, plastic, or canvas has lift on both upper and lower surfaces. The sum of 0.31 lb_f/ft^2 (14.88 N/m^2) is quite low, and based on Table 1, is capable of L:D greater than 100:1.

At a load of 0.31 lb_f/ft^2 (14.88 N/m^2) and 100 m/s (360 kph); the drag is at a rate of 14.88 W/m^2. Energy collection for the solar cells is 135 mW/cm^2 or 1,350 W/m^2. As a result, at 100 m/s the power generation of the solar platform is about 90X the energy needed to sustain flight. Taking into account hours of sunlight and storage efficiency, this translates to about 30X the energy needed for 24/7 flight. At 2X the velocity (720 kph) with 4X the power (4X is a high estimate, the topic is revisited *infra*), the towed panel would still provide about 7.5X the energy needed for 24/7 flight.

Leading and trailing edge effects can be overcome with the same features used in contemporary wing/airfoil designs. A contemporary airfoils' cambered leading edge provides rapid formation of desired surface pressures that would be sustained by flat surfaces along the longitudinal direction. Likewise, fences on sides flat plate airfoils can reduce the cancelling flow of lower-surface higher pressure air with air on the upper surface. Here, CFD and wind tunnel studies are needed for performance estimates.

L:D Dependence on Velocity for Wings – Figure 10 compares the L:D of a flat plate airfoil to a typical wing airfoil. The L:D of the flat plate airfoil has a singularity at $\boldsymbol{\theta}$ = 0. The L:D is also a strong function of $\boldsymbol{\theta}$ (L:D = $\boldsymbol{\theta}^{-1}$). Combined, these two features can cause pitch control and stability problems, especially during takeoff and landing.[3]

Typically-used wing airfoils have a range of $\boldsymbol{\theta}$ where, at the maximum, is <u>approximately</u> constant. This allows flaps to control L:D and creates a situation for stable flight that is relatively easy to control.

The dependence of power needs on $\boldsymbol{v}$ for a typical wing airfoil can be estimated based on solving equations at constant L:D (see Figure 10) and constant lift (i.e. the weight of the aircraft does not change). Using the Equation 5 lift coefficient, Equation 6 is derived with Power ∝ $\boldsymbol{v^3}$.

$$L = 0.5\ A_{WSA}\, C_L\, (\rho\, v_{max}^2) \qquad (\boldsymbol{A_{WSA}} \text{ is wing's wetted surface area}) \qquad (5)$$

$$Power = Dv = \frac{Lv}{CONSTANT} = \frac{0.5\ A_{WSA}\, C_L\, \rho\, v_{max}^3}{CONSTANT} \qquad (6)$$

L:D Dependence on Velocity for Towed Platforms – For a towed flat plate airfoil, the $\boldsymbol{\Delta P}$ term of Equation 1 applies to both drag and lift, and it is set by the load (does not change with velocity). An increase in velocity decreases $\boldsymbol{\theta}$; the total wetted surface area ($\boldsymbol{A_{WSA}}$) is constant; and Equation 7 relates $\boldsymbol{A_{FCS}}$ to $\boldsymbol{A_{WSA}}$. Equation 7 can be used in the Equation 1 integral for drag per Equation 8.

$$A_{FCS} = 0.5\,\theta\, A_{WSA}; \qquad D = \theta\, A_{WSA}\Delta P \qquad (7), (8)$$

Equation 8 identifies that $\boldsymbol{D}$ decreases as $\boldsymbol{\theta}$ decreases, and so, $\boldsymbol{D}$ decreases as $\boldsymbol{v}$ increases. This may seem to defy common sense, but it is actually straight forward logic. Since $\boldsymbol{\Delta P}$ is constant and increasing velocity decreases $\boldsymbol{A_{FCS}}$, the drag of the plate surfaces must decrease with increasing velocity.

Figure 11 shows a platform side cross-section where a large sheet connected to a cambered leading edge and a beveled trailing edge. For prototyping, corrugated plastic is commonly used with RC aircraft and provides a light-weight structure with some rigidity. That leading edge does not have the same drag dynamics as the large midsection sheet, but that leading edge is also relatively small in frontal cross section area for a large sheet. The actual drag profile of towed platform is highly dependent on the size/shape of the cambered leading edge and its size relative to the sheet. As an estimate, the drag of the entire platform is considered to be constant with increasing velocity (versus decreasing for a perfect flat plate). The result is Equation 9, which should be a reasonable correlation for a range of useful combinations of sheets and cambered leading edges.

$$Power \propto v \qquad \text{(for a towed platform)} \qquad (9)$$

[3] The towed platform substantially overcomes stability and control issues for pitch and yaw.

REFERENCES

1. Drela, M. *Making an extraordinary machine better*. 2020; Available from: http://web.mit.edu/drela/Public/ted.pdf.
2. Greitzer, E.M. and H.N. Slater, *Volume 1: N+3 Aircraft Concept Designs and Trade Studies, Final Report*, P.R.f.N.G.R. Center, Editor. 2010, MIT: USA.
3. Mueller, T.J., *Aerodynamic measurements at low Reynolds numbers of fixed wing micro-air vehicles*. 2000: https://apps.dtic.mil/dtic/tr/fulltext/u2/p010760.pdf.
4. Pelletier, A. and T.J. Mueller, *Low Reynolds number aerodynamics of low-aspect-ratio, thin/flat/cambered-plate wings.* Journal of Aircraft, 2000. **37**(5): p. 8.
5. Winslow, J., et al., *Basic understanding of airfoil characteristics at low Reynolds numbers (10^4-10^5).* Journal of Aircraft, 2018. **55**(3): p. 12.
6. Brennen, C.E., *Internet Book on Fluid Dynamics*. 2004: caltech.edu.
7. Winslow, J., et al., *Basic understanding of airfoil characteristics at low Reynolds numbers (10^4-10^5).* Journal of Aircraft, 2018. **55**(3).
8. NASA. *Bernoulli's Equation*. 2020, Available from: https://www.grc.nasa.gov/WWW/K-12/airplane/bern.html.
9. Rothhaar, P.M., W.J. Fredericks, and D.D. North, *Aerodynamically Actuated Thrust Vectoring Devices (US Patent 10,370,100 B2)*. 2019.
10. Spectrolab. *XTE-SF space Qualified Triple Junction Solar Cell*. 2020 [cited 2021; Available from: http://www.spectrolab.com/photovoltaics/XTE-SF%20Data%20Sheet%20_12.23.19.pdf.